Signatures of distinct dynamical regimes in the energy landscape of a glass-forming liquid

Srikanth Sastry*†, Pablo G. Debenedetti* & Frank H. Stillinger‡§

** Department of Chemical Engineering, ‡ Princeton Materials Institute, Princeton University, Princeton, New Jersey 08544, USA*
§ Bell Laboratories, Lucent Technologies, Murray Hill, New Jersey 07974, USA
† Permanent address: Jawaharlal Nehru Center for Advanced Scientific Research, Bangalore 560064, India.

Most materials attain a glassy state at low temperatures under suitable methods of preparation. This state exhibits the mechanical properties of a solid, but shows microscopic structural disorder[1,2]. A comprehensive understanding of the glassy state is, however, still lacking[3]. A widespread assumption is that the non-exponential relaxation processes observed in the dynamics of glasses—and also in protein dynamics, protein folding and population dynamics—are (in common with other manifestations of complex dynamics) strongly influenced by the underlying energy landscape associated with the structural configurations that the system may adopt. But concrete evidence for this in studies of glass formation has been scarce. Here we present such evidence, obtained from computer simulations of a model glass-forming liquid. We demonstrate that the onset of non-exponential relaxation corresponds to a well defined temperature below which the depth of the potential-energy minima explored by the liquid increases with decreasing temperature, and above which it does not. At lower temperatures, we observe a sharp transition when the liquid gets trapped in the deepest accessible energy basin. This transition temperature depends on the cooling rate, in a manner analogous to the experimental glass transition. We also present evidence that the barrier heights separating potential-energy minima sampled by the liquid increase abruptly at a temperature above the glass transition but well below the onset of non-exponential relaxation. This identification of a relationship between static, topographic features of the energy landscape and complex dynamics holds

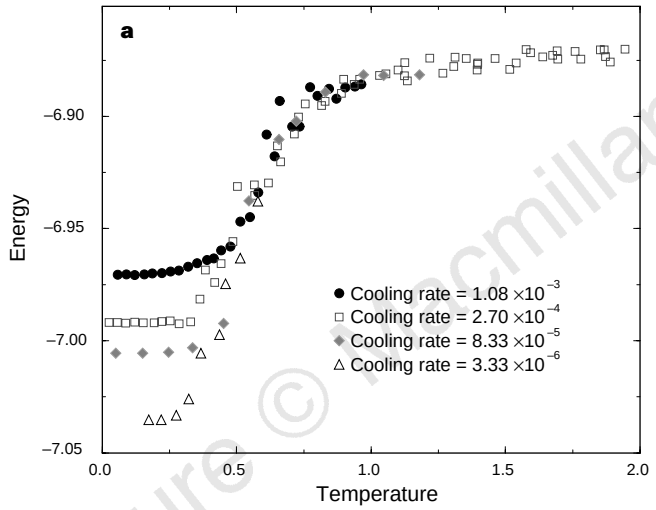

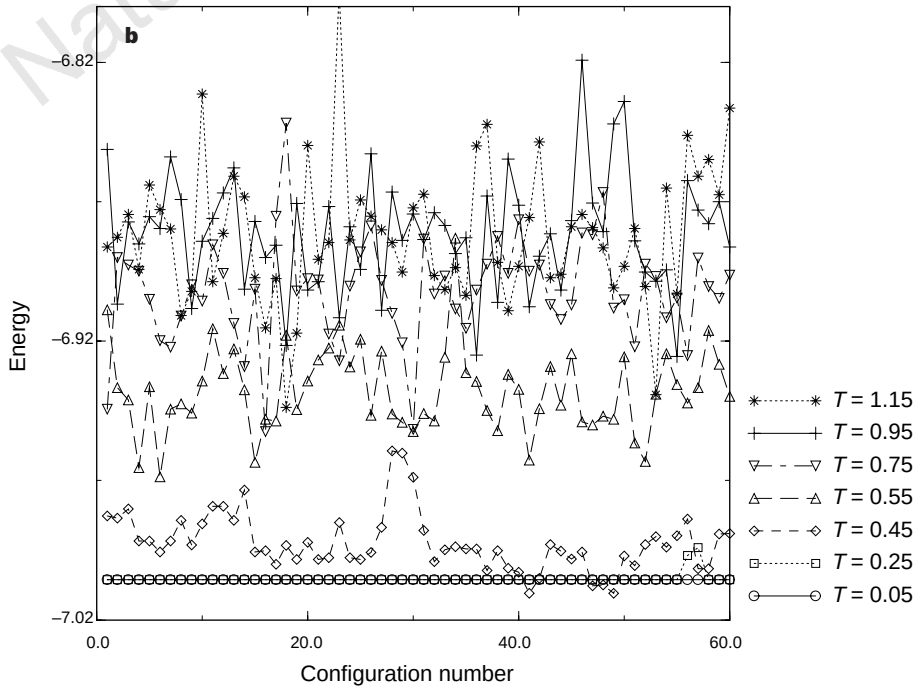

Figure 1 Molecular dynamics simulations of a binary Lennard–Jones mixture[21]. 80% of the particles are of type A, 20% are type B, and Lennard–Jones parameters are $\epsilon_{AA} = 1.0$, $\epsilon_{AB} = 1.5$, $\epsilon_{BB} = 0.5$, $\sigma_{AA} = 1.0$, $\sigma_{AB} = 0.8$ and $\sigma_{BB} = 0.88$. All quantities are in reduced units: length in units of σ_{AA}, temperature in units of ϵ_{AA}/k_B, and time in units of $(\sigma_{AA}^2 m/\epsilon_{AA})^{1/2}$, where m is the mass of the particles. The density ρ in all cases is 1.2. The calculated pressures for the system remain positive except for $T < 0.06$, much below temperatures where the system forms a glass in all cases studied. The Lennard–Jones potential, with a quadratic cut-off and shifting of the potential at $r_c^{\alpha\beta} = 2.5\sigma_{\alpha\beta}$ (ref. 29), $\alpha, \beta \in A, B$ is used. Our cut-off procedure results in a potential minimum value which is ~4% smaller than that in ref. 21. The time step is $dt = 0.003$. Each run was initialized by equilibration at a high temperature, followed by equilibration and data collection runs at a series of temperatures. The run length at each temperature, together with the number of temperatures chosen, determines the cooling rate. Equilibration was done at constant temperature by periodic rescaling of the velocities of particles. Data collection runs were done at constant energy. Local-energy minimization was performed for a subset of configurations generated at each temperature. Data, as well as those in Figs 3 and 4, are from simulations of 256 particles. **a**, The average of the minimum energies per particle. Each data point represents an average over 100 inherent structures, except for cooling rate 8.33×10^{-5}, where 60 configurations were used. The three lower cooling-rate data were obtained from a single run; for the highest cooling rate, the data were averaged over four different cooling runs (25 inherent structures were sampled in each case) to reduce the noise. For temperatures $T = 3.0$, 4.0 and 5.0, the average energies are –6.868, –6.872 and –6.867 respectively, confirming that at high temperatures ($T > 1.0$) the inherent-structure energies reach a constant value independent of temperature. **b**, Individual minimum energies for the configurations at cooling rate 8.33×10^{-5}. At high and intermediate temperatures, these individual energies cover a broad range, and only show a gradual trend towards lower values as the temperature is lowered. A qualitative difference is apparent at low temperatures, with the sampled energies becoming narrowly distributed around the average values. The statistical independence of individual points, however, varies strongly with temperature, particularly as these data represent a single cooling run.

the promise of a clearer, possibly thermodynamic, understanding of the glass transition.

Glasses can be formed in numerous ways[4]. The term 'glass transition', however, is commonly used to designate the disappearance of structural relaxation in a liquid on cooling to low temperatures; the material then becomes rigid, while retaining microscopic structural disorder. Alhough it is conventional to speak of a glass transition temperature, T_g, the experimentally determined T_g of a material depends on how fast the liquid is cooled[1]. The possible existence of an underlying thermodynamic transition remains open, and a topic of great interest[5–7]. At low temperatures, in addition to a rapid decrease of relaxation rates, a glass-forming liquid exhibits 'complex dynamics' such as non-exponential relaxation[2], breakdown of the Stokes–Einstein relation[8,9] and translation–rotation decoupling[10]. The microscopic disorder, complex dynamics and loss of relaxation at finite temperature observed in glass-forming liquids find analogies in various other 'complex systems', most notably spin glasses[11].

An appealing approach for understanding complex dynamics is to consider the influence of a system's 'energy landscape' on the relaxation processes it displays[12–14]. The dynamics of the system is viewed as the motion of the 'state point' (described by the coordinates of all particles) in the $3N$-dimensional configuration space, where N is the number of particles. The potential energy of the system, a function of particle coordinates, defines a complicated $3N$-dimensional surface or 'landscape'. We may partition the configuration space into 'basins', such that a local minimization of the potential energy maps any point in a basin to the same minimum. The properties of the system at a given temperature are dictated by the basins sampled and their mutual accessibility. At high temperatures, kinetic energy permits access to most basins. At lower temperatures, the sampling shifts to lower energies and mutual access among basins becomes subject to considerable 'activation'.

A kinetic description of glassy dynamics that has been much studied, mode-coupling theory (MCT)[15–17], makes no formal contact with the energy landscape picture. In its idealized version, MCT predicts a critical temperature, T_c, where dynamical quantities diverge. It has subsequently been shown[1] that T_c lies above T_g, its singular character arising from approximations of the idealized theory. It has been suggested[18] that activated dynamics, unaccounted for in MCT, begins to be dominant near T_c (we use the term 'activated relaxation' here as commonly used in the supercooled liquids literature, for example in ref. 18, to denote relaxation dominated by episodic particle motions that require overcoming appreciable energy or activation barriers). Further, it has been suggested that T_c demarcates temperatures where the system explores deeper regions of the potential-energy surface from those at which it has access to all regions[19]. But despite the importance of the landscape paradigm, quantitative measures of the manner in which a liquid samples the potential-energy landscape are scarce.

We study a binary mixture of particles interacting via the Lennard–Jones potential, originally proposed as a model for $Ni_{80}P_{20}$ (ref. 20), and widely used as a model glass-former in computer simulations[21,22]. We perform molecular dynamics simulations at constant volume, from very high to deeply supercooled temperatures, each set of simulations being carried out at a given cooling rate. We perform a local potential-energy minimization for selected configurations. The resulting energy-minimum configurations (called inherent structures[23]) serve as markers of the configuration space explored by the system at any given temperature. Although most experimental studies of glass formation are done at constant pressure, the phenomenology has been observed to remain unchanged when volume is held constant instead[24,25].

In Fig. 1a we show the temperature-dependent average energies of the inherent structures, for four different cooling rates. At high temperature ($T > 1.0$), the energies do not change significantly with temperature. Between $T \approx 1.0$ and $T = 0.3$–0.4, the energies decrease progressively. Below this range of temperatures, the energies are constant once again. Figure 1b shows that at high temperature the system explores a broad range of minimum energies and

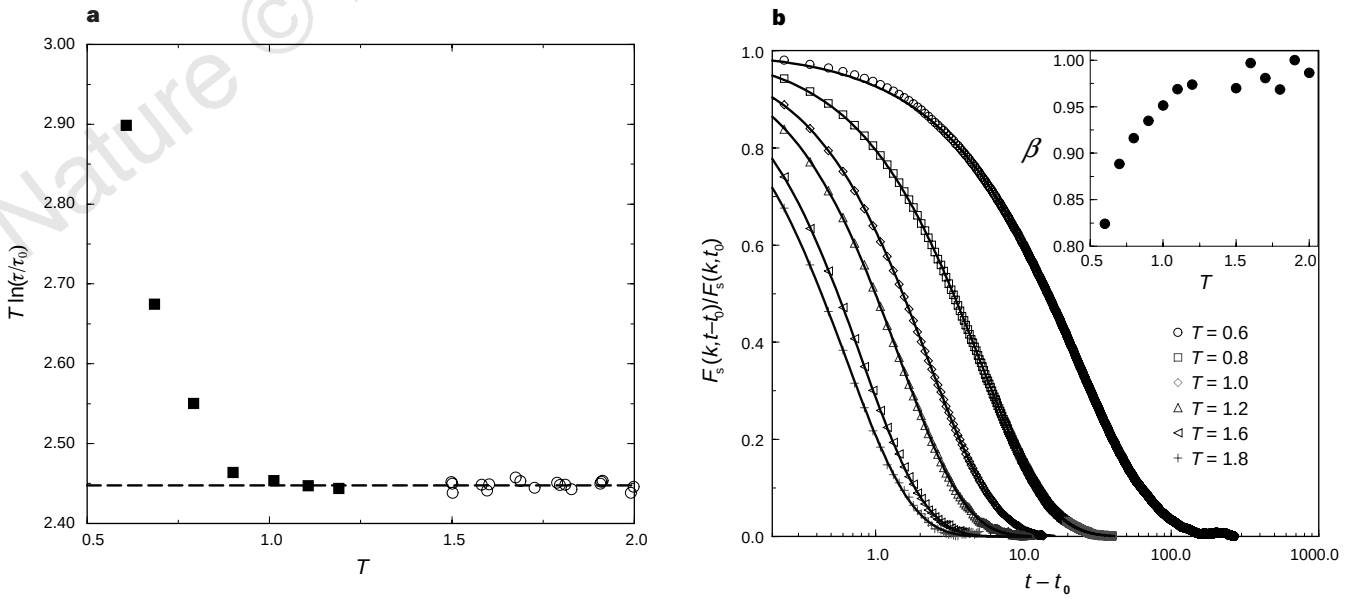

Figure 2 Transition from high-temperature behaviour to the 'landscape-influenced' regime where non-exponential relaxation sets in. **a**, Relaxation times from the space Fourier transform $F_s(k,t)$ of the self part of the van Hove correlation function (self intermediate scattering function). The wavevector is $k = 7.21\bar{\sigma}_{AA}^{-1}$, close to the first peak of the static structure factor. The infinite temperature relaxation time τ_0 is obtained by fitting $\tau(T)$ values for $T = 1.5$–2.0 (circles) to an Arrhenius form. The quantity plotted, $T\ln(\tau/\tau_0)$, is constant when τ displays Arrhenius behaviour. Deviation from the constant, high-temperature value is seen around $T = 1.0$ (squares). **b**, The self intermediate scattering function displayed with a shift in the time origin to $t_0 = 1.2$, and normalized to the value at t_0. We use this transformation as a convenient procedure to eliminate the gaussian time dependence at short t (ref. 26). The fits are to the stretched exponential form in equation (2). The inset shows the exponent values $\beta(T)$. As a check, we fitted our data to a simple exponential form, and confirmed that above $T = 1.0$ fits were satisfactory, whereas below $T = 1.0$, the fits showed systematic deviations indicating slower than exponential decay. Data are from simulations of 1,372 particles.

that on lowering the temperature, the sampling becomes progressively biased towards lower energies, becoming more narrowly distributed around the average values.

We expect a qualitative change in the dynamics below the crossover at around $T = 1.0$, based on the observed T-dependence of the inherent-structure energies. To evaluate this expectation, we calculate the self intermediate scattering function $F_s(k,t)$ (ref. 26), the Fourier transform at wavevector k of the van Hove self-correlation function

$$G_s(r,t) = \frac{1}{N}\sum_{i=1}^{N}\langle\delta(|\mathbf{r}_i(t) - \mathbf{r}(0)| - r)\rangle \quad (1)$$

which describes the probability of finding at time t a particle at distance r from its location at $t = 0$. We define a relaxation time $\tau(T)$ as the time when $F_s(k,t) = 1/e$. At high temperature, $\tau(T)$ displays the Arrhenius form, $\tau = \tau_0 \exp(E/k_B T)$ (k_B is the Boltzmann constant and E is the activation energy, a constant). As shown in Fig. 2a, this simple behaviour breaks down around $T = 1.0$, below which the measured τ are progressively higher than extrapolations from higher temperatures. This behaviour corresponds to that of 'fragile liquids' in the strong–fragile classification[18]. At high temperatures, the time dependence of $F_s(k,t)$ is exponential, whereas at lower temperatures, the Kohlrausch–Williams–Watts stretched exponential form

$$F_s(k,t) = \exp\left[-\left(\frac{t}{\tau(T)}\right)^{\beta(T)}\right] \quad (2)$$

provides a good fit to the long-time behaviour. In equation (2) $\beta(0 < \beta < 1)$ is a number that quantifies the deviation from strict exponential behaviour. We consider the functions $[F_s(k, t - t_0)]/(F_s(k, t_0), t > t_0$, which we fit to the form in equation (2) to quantify their long-time behaviour. The fits and the values for $\beta(T)$ are shown in Fig. 2b, which shows that $\beta(T)$ drops considerably below 1 as the temperature decreases below $T = 1.0$. We call this the 'landscape-influenced' regime. These results demonstrate the connection between the onset of 'slow dynamics' and a change in the manner of exploration of the potential-energy landscape. Such a connection has been proposed before[4,12–14], but our results, we believe, constitute its first clear demonstration.

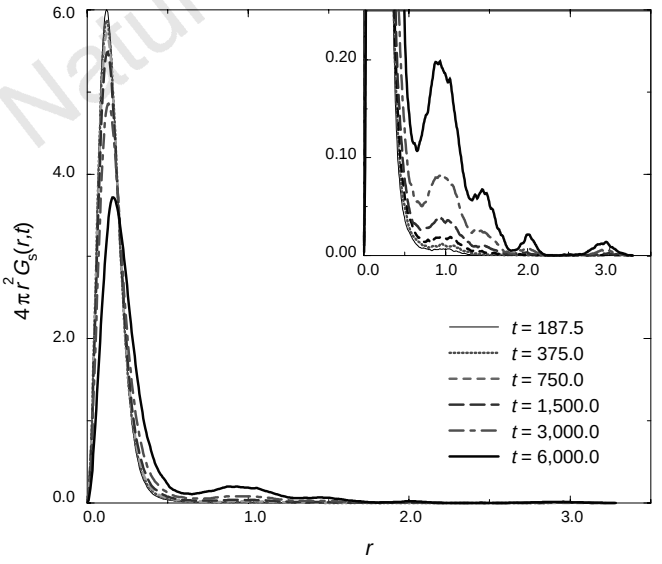

Figure 3 The van Hove self-correlation function for $T = 0.425$, shown for different values of t. Inset shows a magnification of the secondary peaks corresponding to activated events. Such secondary peaks have previously not been observed for $T > 0.466$ in the model we study[21], but have been observed in a related model[28] at low temperatures.

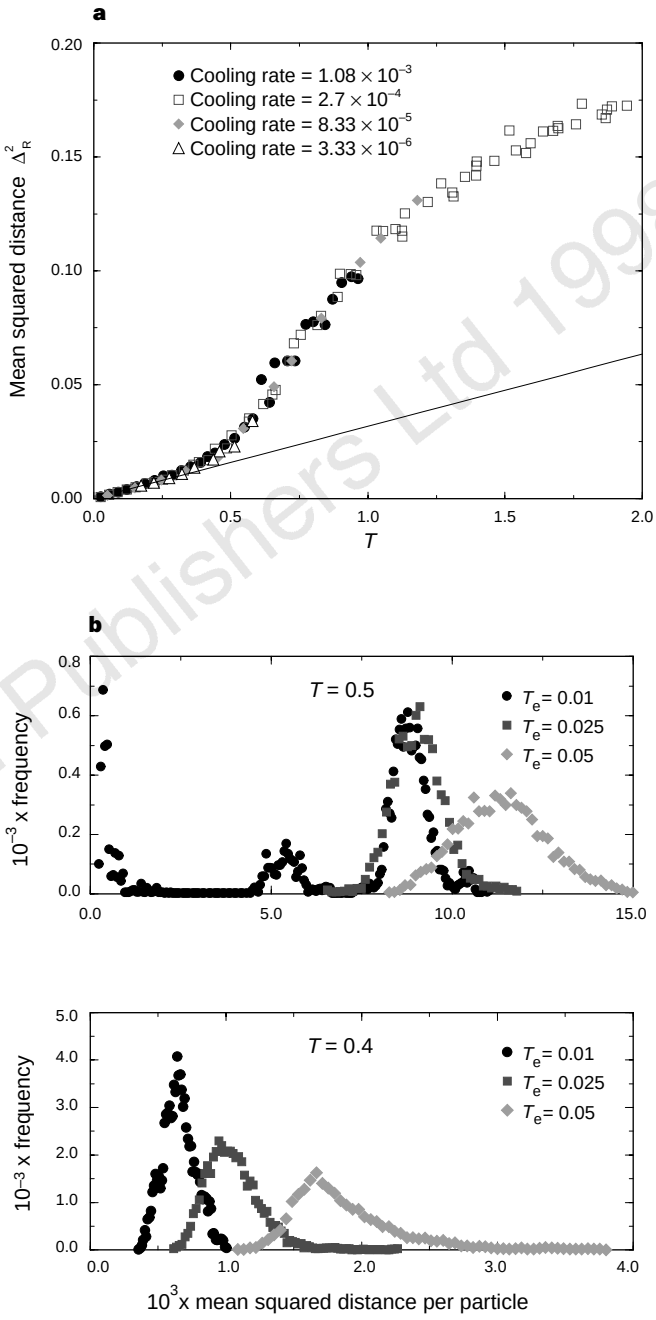

Figure 4 Onset of the 'landscape-dominated' regime at $T \approx 0.45$. **a**, The average mean-squared distance per particle Δ_R^2 between a typical liquid configuration and the corresponding inherent structure. For a quadratic minimum, Δ_R^2 is equivalent to average squared displacements due to harmonic vibrations, and hence proportional to the temperature. The reference straight line, whose slope equals that of mean-squared distances for harmonic vibrations around an inherent structure for $T = 0.175$, cooling rate $= 3.33 \times 10^{-6}$, suggests that at low temperatures Δ_R^2 indeed arises from harmonic vibrations. The observed sharp deviation from the low-temperature straight line thus suggests the onset of anharmonicity in the sampled basins. **b**, Distribution of squared distances sampled when an inherent structure is excited to energies labelled by T_e, the temperature corresponding to the kinetic energy of excitation. The subscript 'e' distinguishes this 'excitation' temperature from that of the liquid from which the inherent structures are obtained. We note that all values of T_e are substantially lower than the glass transition temperature T_g. For inherent structures obtained from the higher temperature $T = 0.5$, the system finds basins of nearby energy minima for all but the lowest level of excitation. For the lower temperature $T = 0.4$, this is not the case, and the system remains confined to the basin of the initial inherent structure.

Examination of the internal-energy and pressure curves for the liquid from which the inherent structures are obtained reveals that the sharp low-temperature break in the inherent-structure energy curve corresponds to T_g as commonly estimated in simulations[27]. Thus, calculation of inherent-structure energies offers an alternative way for locating the glass transition temperature in computer simulations. The advantage of our procedure is that the signature of the transition is very sharp, although it requires considerable additional computation. Based on the differences between curves for successive cooling rates, we note that the system begins to fall out of equilibrium well above the low-temperature plateau.

The temperature range slightly above T_g, where inherent-structure energies show a gradual change with temperature, includes the temperature where MCT predicts a divergence in relaxation times ($T_c \approx 0.435$ in ref. 21). Instead of this divergence, one observes deviations from MCT predictions as T_c is approached, possibly due to 'activated processes'[12,13,18]. These lead to secondary peaks in the van Hove self-correlation function[21,28], resulting from rare jumps of particles over distances roughly equal to interparticle separations. Figure 3 shows $G_s(r,t)$ for $T = 0.425$. Secondary peaks appear at positions $r \approx 1.0$, 1.44, 2.0 and 3.0, whereas no such distinct peaks are found at higher temperatures. Thus, at $T = 0.425$, the system shows evidence of activated dynamics. We call this the 'landscape-dominated' regime.

Figure 4a shows the mean-squared distance Δ_R^2 between a typical liquid configuration and the corresponding energy minimum, defined as $\Delta_R^2 = (1/N)\Sigma(\mathbf{r}_i - \mathbf{r}_i^{(q)})^2$, where $\mathbf{r}_i$ are the coordinates of particles i, and $\mathbf{r}_i^{(q)}$ are coordinates in the corresponding inherent structures. A crossover from roughly linear behaviour at low temperatures to a more rapid increase occurs at around $T = 0.45$. In addition, the dependence on Δ_R^2 of the path length traversed during energy minimization also displays a break at $T \approx 0.45$ (data not shown), indicating an increased roughness of the landscape sampled at higher temperatures. These observations indicate a sharp change in the local topography of the sampled landscape around $T = 0.45$, which is close to the previous estimate of T_c (ref. 21).

Further insight is obtained by exciting inherent structures obtained from a given temperature to various energies (with kinetic energies corresponding to very low excitation temperatures, T_e) and monitoring the distribution of distances from the starting inherent-structure configuration, which are shown in Fig. 4b. At $T = 0.4$, the location of the peaks of the distribution is roughly proportional to T_e. At $T = 0.5$, on the other hand, even at very low excitation, the system finds other basins, as evidenced by multiple peaks and substantially higher sampled distances. This indicates that whereas at high temperature the system explores a part of the landscape with low barriers between energy minima, at lower temperatures it explores minima with substantially higher energy barriers. □

Received 29 December 1997; accepted 1 April 1998.

1. Debenedetti, P. G. *Metastable Liquids* (Princeton Univ. Press, Princeton, 1996).
2. Ediger, M. D., Angell, C. A. & Nagel, S. R. Supercooled liquids and glasses. *J. Phys. Chem.* **100,** 13200–13212 (1996).
3. Anderson, P. W. Through the glass lightly. *Science* **267,** 1615 (1995).
4. Angell, C. A. Formation of glasses from liquids and biopolymers. *Science* **267,** 1924–1935 (1995).
5. Kauzmann, W. The nature of the glassy state and the behavior of liquids at low temperatures. *Chem. Rev.* **43,** 219–256 (1948).
6. Gibbs, J. H. & DiMarzio, E. A. Nature of the glass transition and the glassy state. *J. Chem. Phys.* **28,** 373–383 (1958).
7. Stillinger, F. H. Supercooled liquids, glass transitions, and the Kauzmann paradox. *J. Chem. Phys.* **88,** 7818–7825 (1988).
8. Heuberger, G. & Silescu, H. Size dependence of tracer diffusion in supercooled liquids. *J. Phys. Chem.* **100,** 15255–15260 (1996).
9. Chang, I., Fujara, F., Geil, B., Heuberger, G. & Silescu, H. Translational and rotational molecular motion in supercooled liquids studied by NMR and forced Rayleigh scattering. *J. Non-Cryst. Solids* **172–174,** 248–255 (1994).
10. Cicerone, M. T., Blackburn, F. R. & Ediger, M. D. How do molecules move near T_g? Molecular rotation of six probes in o-terphenyl across 14 decades in time. *J. Chem. Phys.* **102,** 471–479 (1995).
11. Parisi, G. New ideas in glass transitions. in *Proc. Int. Workshop on The Morphology and Kinetics of Phase Separating Complex Fluids* (eds Chen, S. H., Mallamace, F. & Tartaglia, P.) *Il Nuovo Cimento D* (in the press).
12. Goldstein, M. Viscous liquids and the glass transition: a potential energy barrier picture. *J. Chem. Phys.* **51,** 3728–3739 (1969).
13. Goldstein, M. Viscous liquids and the glass transition. VII. Molecular mechanisms for a thermodynamic second order transition. *J. Chem. Phys.* **67,** 2246–2253 (1977).
14. Stillinger, F. H. A topographic view of supercooled liquids and glass formation. *Science* **267,** 1935–1939 (1995).
15. Götze, W. & Sjögren, L. Relaxation processes in supercooled liquids. *Rep. Prog. Phys.* **55,** 241–376 (1992).
16. Bengtzelius, U., Götze, W. & Sjölander, A. Dynamics of supercooled liquids and the glass transition. *J. Phys. C* **17,** 5915–5934 (1984).
17. Leutheusser, E. Dynamical model for the liquid-glass transition. *Phys. Rev. A* **29,** 2765–2773 (1984).
18. Angell, C. A. Perspective on the glass transition. *J. Phys. Chem. Sol.* **49,** 863–870 (1988).
19. Angell, C. A. in *Complex Behavior in Glassy Systems* (eds Rubi, M. & Perez-Vicente, C.) 1–21 (Springer, Berlin, 1997).
20. Weber, T. A. & Stillinger, F. H. Local order and structural translations in amorphous metal-metalloid alloys. *Phys. Rev. B* **31,** 1954–1963 (1985).
21. Kob, W. & Andersen, H. C. Testing mode-coupling theory for a supercooled binary Lennard-Jones mixture: the van Hove correlation function. *Phys. Rev. E* **51,** 4626–4641 (1995).
22. Donati, C., Douglas, J.F., Plimpton, S.J., Poole, P. H. & Glotzer, S. C. String-like cooperative motion in a supercooled liquid. *Phys. Rev. Lett.* **80,** 2338–2342 (1998).
23. Stillinger, F. H. & Weber, T. A. Packing structures and transitions in liquids and solids. *Science* **225,** 983–989 (1984).
24. Angell, C. A. *et al.* in *Slow Dynamics in Condensed Matter: Proc. 1st Tohwa Univ. Int. Symp.* (eds Kawasaki, K., Kawakatsu, T. & Tokuyama, M.) 3–19 (AIP Conf. Proc. 316, Am. Inst. Physics, New York, 1992).
25. Colucci, D. M. *et al.* Isochoric and isobaric glass formation: similarities and differences. *J. Polym. Sci. B: Polym. Phys.* **35,** 1561–1573 (1997).
26. Hansen, J.-P. & McDonald, I. R. *Theory of Simple Liquids* (Academic, London, 1986).
27. Fox, J. R. & Andersen, H. C. Molecular dynamics simulations of a supercooled monoatomic liquid and glass. *J. Phys. Chem.* **88,** 4019–4027 (1984).
28. Wahnström, G. Molecular-dynamics study of a supercooled two-component Lennard–Jones system. *Phys. Rev. A* **44,** 3752–3764 (1991).
29. Stoddard, S. D. & Ford, J. Numerical experiments on the stochastic behavior of a Lennard–Jones gas system. *Phys. Rev. A* **8,** 1504–1512 (1973).

Acknowledgements. We thank C. A. Angell, S. Glotzer, F. Sciortino and H. E. Stanley for discussions. This work was supported by the US Department of Energy and the Petroleum Research Fund.

Correspondence and requests for materials should be addressed to P.G.D. (e-mail: pdebene@pucc.princeton.edu).

Millennial-scale changes in North Atlantic circulation since the last glaciation

Thomas M. Marchitto Jr*, William B. Curry† & Delia W. Oppo†

* *Massachusetts Institute of Technology/Woods Hole Oceanographic Institution Joint Program in Oceanography, Woods Hole, Massachusetts 02543, USA*
† *Woods Hole Oceanographic Institution, Woods Hole, Massachusetts 02543, USA*

Ocean circulation is closely linked to climate change on glacial–interglacial and shorter timescales. Extensive reorganizations in the circulation of deep and intermediate-depth waters in the Atlantic Ocean have been hypothesized for both the last glaciation[1–6] and the subsequent Younger Dryas cold interval[3,6–10], but there has been little palaeoceanographic study of the subtropical gyres[11–13]. These gyres are the dominant oceanic features of wind-driven circulation, and as such they reflect changes in climate and are a significant control on nutrient cycling and, possibly, atmospheric CO_2 concentrations. Here we present Cd/Ca ratios in the shells of benthic foraminifera from the Bahama banks that confirm previous suggestions[11,12] that nutrient concentrations in the North Atlantic subtropical gyre were much lower during the Last Glacial Maximum than they are today (up to 50% lower according to our data). These contrasting nutrient burdens imply much shorter residence times for waters within the thermocline of the Last Glacial Maximum. Below the glacial thermocline, nutrient concentrations were reduced owing to the presence of Glacial North Atlantic Intermediate Water. A high-resolution Cd/Ca record from an intermediate depth indicates decreased nutrient concentrations during the Younger Dryas interval as well, mirroring opposite changes at a nearby deep site[3,9]. Together, these observations suggest that the formation of deep and intermediate waters—North Atlantic Deep Water and Glacial North